Eur. Phys. J. Plus (2024) 139:619
https://doi.org/10.1140/epjp/s13360-024-05437-z

THE EUROPEAN PHYSICAL JOURNAL PLUS

Regular Article

Optimizing quantum refrigerators with a qubit on the hot side

J. J. Fernández[a]

Departamento de Física Fundamental, Universidad Nacional de Educación a Distancia (UNED), 28040 Madrid, Spain

Received: 11 January 2024 / Accepted: 8 July 2024

Abstract We study the performance of one-qubit quantum and semiclassic refrigerators with the qubit on the hot side. We obtain the cooling power and the Ω function. We discover that the quantum refrigerators perform differently to classic ones. We also prove that even in the high-temperature limit, where the semiclassic version of the refrigerator is valid, the results of the optimization are different to those obtained by optimizing classic refrigerators.

Quantum Thermodynamics (QTD) is the branch of Quantum Mechanics (QM) dealing with the study of engines that produce work on the nanoscale [1]. A general definition of a quantum thermodynamic machine says *quantum machines are thermal engines that work under the time evolution rules that are dictated by the QM*. This definition is very suitable since it extends the current definitions of quantum heat engines (QHEs) in such a way that it allows quantum refrigerators (QRs) to be included.

In the last 70 years, some attention to QHEs and QRs has been devoted. In recent years, furthermore, research in the field of QTD has become quite specialized. This means that we can define three types of jobs within this field. In a first group, we find jobs on the basis of QTD. In them, the authors study the basis of the QTD by proving how the basic principles of thermodynamics arise from the laws of QM. In a second group, we find works that explore the general properties of thermodynamic quantum systems, trying to understand them and to obtain some properties such as energy fluxes Q_h and Q_c, the system entropy change ΔS, and other thermodynamic properties [1–8]. In them, the authors also use the results to asses or to discard conjectures about the similarity between QTDs and classic thermodynamics. Finally, we find another set of works that are, somehow, more applied: those studying how a concrete quantum thermodynamic system performs in the best possible way. Among the works belonging to the last group, we find works studying how much work is produced by a quantum system or how a classic thermodynamic cycle can be reproduced using a concrete quantum system. In this group, we also find other works that are even more applied. In them, the authors choose a concrete version of a quantum machine and, using the Finite-time Thermodynamics (FTTD) [9–30], obtain its relevant thermodynamic functions using, to calculate the relevant fluxes in the machine, the theory of open-quantum systems [31–35].The authors also optimize the performance of the engines [36–39].

As it is seen looking at the references [36–39], the strategy mentioned in the previous paragraph has only been used to study qubit-based QHEs, but it has not been used to study qubit-based QRs. From a theoretical standpoint, there is no reason not to extend the works on qubit-based QHEs to qubit-based QRs. In this work, we start with this extension proposing the study of a one-qubit QR (OQR) with the qubit on the hot side, see Fig. 1. Doing this, we prove that the methods used in [36–39] to study QHEs are also applicable to the study of QRs and, by extension, to other thermodynamic engines. Moreover, and from a more practical standpoint, the study presented in this work also serves to understand whether QRs perform as classic refrigerators or not, thus also opening the way to carry out studies on quantum systems that could work as refrigerators on the nanoscale. To achieve this last target, we study here the cooling power Q_c and the Ω function (Ω) [27] of OQRs. When doing it, we also comment on the effects of the strength of the coupling between the qubit and the thermal baths, thus following the research lines scoped in [40–42]. Finally, it is worthy to mention that our OQR is, somehow, similar to other devices that are studied in the literature [43, 44], which makes our study (i) comparable and (ii) demonstrates that the study of this type of machines is essential to improve our understanding of the fundamental principles of QTD.

The work is organized as follows: In Sect. 1, we present the OQR under study in this work. We start calculating (by means of the solutions of the Lindbland equation [45]) the relevant heat fluxes of the machine. Then we deduce, using the techniques of the FTTD [9–30], Q_c and Ω. In Sect. 2, we optimize the performance of different OQRs. First, we optimize them considering that the temperatures T_h and T_c of the hot and cold baths are fixed to understand the performance of OQRs that work coupled to fixed environments. Then, we carry a more general investigation considering OQRs of different Carnot COPs (ε_C). This second kind of studies allow us to optimize the performance of OQRs working in different environments. In Sect. 3, we explore the behavior of the OQR in the limit in which E and T_c satisfy $E/T_c \ll 1$. Our intention is to understand whether, in this limit, OQRs reduce to their classic counterpart or not. It is also our objective to study how semiclassic refrigerators can be optimized, which are their optimal

[a] e-mail: jjfernandez@fisfun.uned.es (corresponding author)

Published online: 15 July 2024

working properties and how do they compare to those of classic refrigerators. We end this work with a summary of our findings and a perspective of future work.

1 One-qubit quantum refrigerator with the qubit on the hot side

Figure 1 depicts the OQR that is studied in this work. It has two baths filled with bosons on its extremes. One of them is called hot bath and is characterized by the temperature T_h. The other one is called cold bath, and it is characterized by the temperature T_c. Both baths are filled with bosons and have the spectrum of an oscillator. The bath of temperature T_c is in perfect contact with a Carnot Refrigerator (CR) that extracts power from it and rejects power to the bath of temperature T_1. This bath is connected with that of temperature T_h via a qubit of energy E. Thus, T_c, T_h and T_1 in our engine satisfy $T_1 > T_h > T_c$.

In our engine, the amount of energy that passes from the bath of temperature T_1 to that of temperature T_h is controlled by the qubit of energy E. As it has been proven in previous works [36–39], controlling the energy E of the qubit, the amount of energy that ends in the bath of temperature T_h is increased (if E gets bigger) or decreased (if E gets smaller).

In order to calculate the energy fluxes circulating through the OQR, we assume that the Hamiltonian of the qubit is

$$H = \frac{E}{2}\begin{pmatrix} 1 & 0 \\ 0 & -1 \end{pmatrix}. \tag{1}$$

The energy levels of the qubit are $\pm E/2$, and its state is characterized by the 2×2 time-dependent density matrix $\rho(t)$. The time evolution of $\rho(t)$ is given by the Lindbland equation [45]:

$$\frac{d\rho(t)}{dt} = -i[H, \rho(t)] + \mathcal{D}_h[\rho] + \mathcal{D}_1[\rho]. \tag{2}$$

The first term on the right hand side of Eq. (2) gives the unitary part of the evolution and expresses the quantum nature of our qubit. The other two terms, $\mathcal{D}_h[\rho]$ and $\mathcal{D}_1[\rho]$, are known as *the dissipators* and introduce in the equation the interactions between the qubit and the baths of temperatures T_h and T_1. In OQRs, the energetic spectra of the cold and hot baths are those of a harmonic oscillator. Thus, the dissipators have the following structure:

$$\mathcal{D}_i = \Gamma_i\left[n_i\left(\sigma^+\rho\sigma^- - \frac{1}{2}\{\sigma^-\sigma^+, \rho\}\right) + \bar{n}_i\left(\sigma^+\rho\sigma^- - \frac{1}{2}\{\sigma^-\sigma^+, \rho\}\right)\right]. \tag{3}$$

Here, $i = h$ stands for the dissipator connecting the qubit to the reservoir of T_h and $i = 1$ for the one that connects the qubit and the reservoir of T_1. Following what is done in previous works, we use Barrow's [46] approximation. So, we consider that the thermal couplings Γ_1 and Γ_h are constant in each calculation to be carried out. In Eq. (3), the creation and annihilation operators are $\sigma^+ = |1\rangle\langle 0|$ and $\sigma^- = |0\rangle\langle 1|$. The occupation of the bath i ($i = 1, h, c$) at the energy E is $n_i = [\exp(\beta_i E) - 1]$, assuming that the baths are filled with bosons. In n_i, $\beta_i = 1/T_i$ is the temperature inverse. As in previous works [36–39], we use Planck's units. This means that for us, $k_B = \hbar = 1$ and that we assume that the dissipation constants Γ_1 and Γ_h, the temperatures T_1, T_h and T_c and the energy E have no units.

It is also interesting to note that for us, a concrete OQR is defined once the constants Γ_1 and Γ_1 and the temperatures T_h and T_c are given. When the OQR is defined, we calculate the energy flux $Q_h = \mathrm{Tr}[H\mathcal{D}_h[\rho]]$ going from the reservoir of temperature T_1 to that of temperature T_h [36]. As the reservoir of T_1 remains at this temperature all the time, we know that Q_1, the energy rejected from the CR, is $Q_1 = \mathrm{Tr}[H\mathcal{D}_h[\rho]]$, i.e., we know that $Q_h = Q_1$. For OQRs working in steady state, Q_h and Q_1 are obtained by

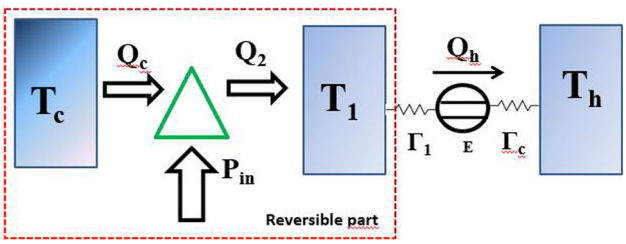

Fig. 1 One-qubit quantum refrigerator (OQR). In the extremes of the OQR, we find two thermal baths of temperatures T_h and T_c. They are filled with bosons, and their energy spectrum is that of an oscillator. The reservoir of temperature T_1 has the same structure, and it is connected to the reservoir of temperature T_h by a qubit of energy E. Between the reservoirs of temperatures T_c and T_1, a CR extracts energy from the reservoir of temperature T_c, injects it into the reservoir of temperature T_1 and accepts power P_{in}

doing $d\rho(t)/dt = 0$ in Eq. (2) and using the solution $\bar{\rho} = (1 + a^z\sigma^z)/2$ [36] in Eq. (3). Here, $a^z = (\Gamma_h + \Gamma_1)/(\Gamma_h S_h + \Gamma_1 S_1)$, $S_h = 2n_h + 1$ and $S_1 = 2n_1 + 1$ are two functions of the occupations of the reservoirs. Using $\bar{\rho}$, we calculate

$$Q_h = \gamma_h E(n_1 - n_h), \tag{4}$$

where $\gamma = \Gamma_h\Gamma_1/(\Gamma_h S_h + \Gamma_1 S_1)$. We note that $Q_h \geq 0$ since $n_1 \geq n_h$, and that this happens because $T_1 \geq T_h$.

Figure 1 shows that at the core of the OQR, a CR boosts the cooling process. The CR works between two isotherms of temperatures T_c and T_1, with $T_c < T_1$, so its COP is $\varepsilon = T_c/(T_1 - T_c)$. Since in the OQR, $T_1 \geq T_h$, we know that ε is always bigger than the Carnot COP $\varepsilon_C = T_c/(T_h - T_c)$, defined by the temperatures of the baths placed on the OQR extremes. Moreover, since we know that the CR works reversibly, we realize that $Q_1/T_1 = Q_c/T_c$. This equality is used to calculate

$$Q_c = \frac{T_c}{T_1}\gamma_h E(n_1 - n_h). \tag{5}$$

Once we have Q_c, we use the energy conservation principle $Q_c + P_{in} = Q_h$ to calculate P_{in},

$$P_{in} = \gamma_h E(n_1 - n_h)\left[\frac{T_1}{T_c} - 1\right]. \tag{6}$$

Moreover, as $n_1 > n_h$ and $T_c/T_1 > 1$, we know that $P_{in} > 0$. Finally, having Q_c, Q_h and P_{in}, we calculate the OQR COP,

$$\varepsilon = \frac{(T_c/T_1)\gamma E(n_1 - n_h)}{\gamma E(n_1 - n_h) - (T_c/T_1)\gamma E(n_1 - n_h)} = \frac{T_c}{T_1 - T_c}. \tag{7}$$

and the Ω-function $\Omega = \dfrac{2\varepsilon - \varepsilon_C}{\varepsilon} Q_c$ [47]. Ω, in terms of the parameters defining the OQR, is

$$\Omega = \gamma_h E \frac{2T_h - T_c - T_1}{T_h - T_c}\frac{T_c}{T_1}(n_1 - n_h). \tag{8}$$

2 Optimizations

2.1 Fixed T_h and T_c

We start studying Q_c and Ω, see Eqs. (5) and (8), in terms of ε to understand the working properties of OQRs. To prove the generality of our results, we present results for two combinations of temperatures (A) $T_h = 10$ and $T_c = 2$ and (B) $T_h = 20$ and $T_c = 2$. In both cases, we use $E = 10$. For the set (A), $\varepsilon_C = 1/4$, and for the set (B), $\varepsilon_C = 1/9$. Using Fig. 2, we analyze the behavior of Q_c in terms of ε. We find the following results: (i) Q_c is zero for $\varepsilon = 0$ and $\varepsilon = \varepsilon_C$. (ii) It is positive for every other value of $\varepsilon \in (0, \varepsilon_C)$ and (iii) reaches a maximum for $\varepsilon = \varepsilon^*$. ε^* is always different to 0 and ε_C. The concrete value of ε^* is different for each OQR and changes with E, T_h and T_c. It also changes with Γ_h and Γ_1.

Our results for Q_c show that its curve, in terms of ε, is similar to those of classic refrigerators. Thus, Q_c has maximum for $\varepsilon \neq 0$, η_C and $\varepsilon \in (0, \eta_C)$. We also find that while in classic refrigerators, ε only depends on T_h and T_c, in OQRs, ε depends on T_h, T_c E, Γ_h and Γ_1. To better check this result and to prove the dependence of Q_c on E more clearly, we present in Fig. 3 the curve of Q_c versus ε of OQRs where the hot and cold heat reservoirs have the temperatures $T_h = 10$ and $T_c = 2$. For completeness, we present results for OQRs of qubit energies $E = 10$, 15, 20. We appreciate that the maximum value Q_c^{max} of Q_c is different for the three OQRs. We also see that the value ε^* of ε, for which $Q_c = Q_c^{max}$, is different for different values of E. This means that in OQRs, Q_c

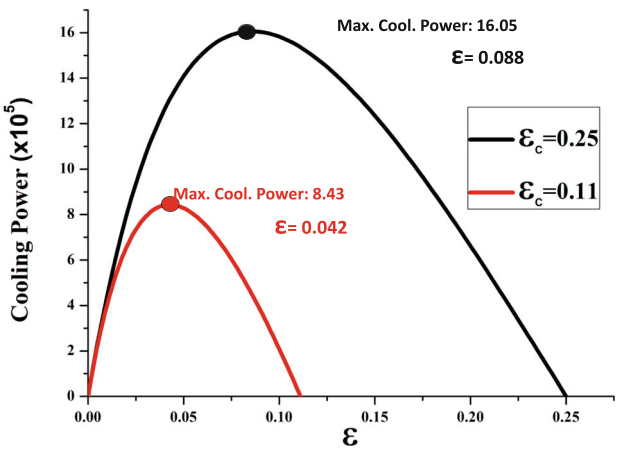

Fig. 2 Cooling power Q_c calculated for two different OQRs with $\varepsilon_C = 0.25$ (black line) and $\varepsilon_C = 0.11$ (red line)

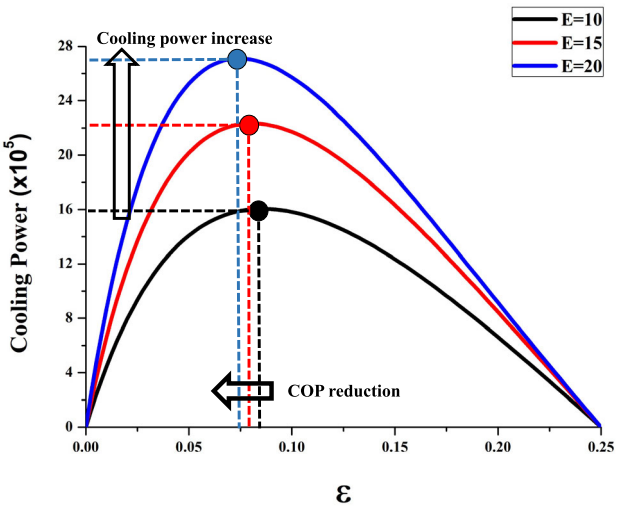

Fig. 3 Cooling power Q_c calculated for three different OQRs with $\varepsilon_C = 0.25$. The OQRs qubit energies are $E = 10$ (black line), $E = 15$ (red line) and $E = 20$ (blue line)

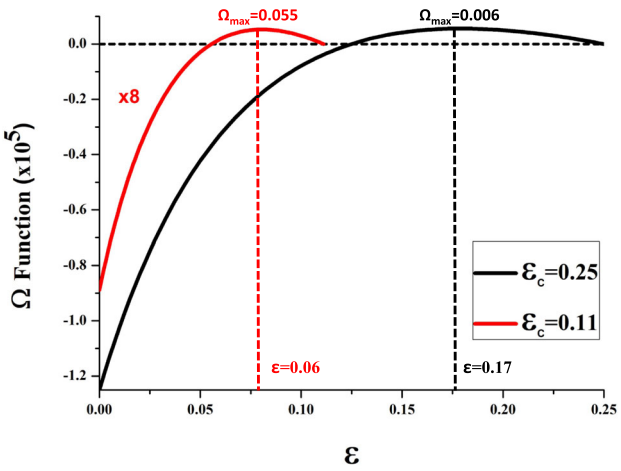

Fig. 4 Ω function versus ε. We present results for two different OQRs. One of them has $\varepsilon_C = 0.25$ (black line), and the other one has $\varepsilon_C = 0.11$ (red line)

is modified when E changes. This result is important, showing that OQRs work differently to classic refrigerators, as in the last ones, Q_c^{max} and ε^* only change with T_h and T_c and that it does not change with the value of the heat resistance [20]. Let us remember that in classic refrigerators, neither Q_c^{max} nor ε^* depend on the thermal resistances placed on the hot branch of the refrigerator [20].

Doing calculations for different values of T_h, we find that Q_c^{max} increases with T_h and that ε^* decreases with this temperature. We show this presenting results for $T_c = 2$ and $\varepsilon_C = 0.25$ ($T_h = 5T_c$)/$\varepsilon_C = 0.11$ ($T_h = 11T_c$) in Fig. 3. We highlight that the results presented in the figure are general and that similar results are found for other values of ε_C.

Figure 4 helps us to study the behavior of Ω in terms of ε. Ω is negative in the limit $\varepsilon \to 0$, increases when ε grows until reaching a maximum and then decreases to zero when $\varepsilon \to \varepsilon_C$. This behavior is general for every value of ε_C, and it is, of course, found in the two curves of our figure (corresponding to $\varepsilon_C = 0.11$ and $\varepsilon_C = 0.25$). The value $\varepsilon^\dagger$ of ε for which Ω is maximum depends on ε_C indicating that it depends on T_h and T_c. In the concrete cases studied, we find $\Omega^{max}(\varepsilon_C = 0.11) = 0.055$, $\Omega^{max}(\varepsilon_C = 0.25) = 0.006$, $\varepsilon^\dagger(\varepsilon_C = 0.11) = 0.06$ and $\varepsilon^\dagger(\varepsilon_C = 0.25) = 0.17$. This figure also allows us to understand the results of optimizations using the Ω-criteria on OQRs showing that the result of the optimization is a maximization of the cooling power (see Fig. 3), restricted with the condition of doing the machine to work at a (real) COP that is under the Carnot one. We highlight that in the optimizations carried out here in particular, and in those that can be done in general, the optimizations using the Ω-criterium result in working configurations where the cooling power is not maximum (see the points corresponding to $\varepsilon = 0.06$ and $\varepsilon = 0.17$) in Fig. 3, but that it has a value that is near to the maximum. It is very important to stress here that the result found for Ω is clearly different to the one found in classic refrigerators, where it is found that Ω increases with ε, so Ω has no maximum. Thus, we can affirm that the behavior of OQRs and classic refrigerators is different.

To understand the behavior of Ω^{max} and $\varepsilon^\dagger$ with E, we fix $\varepsilon_C = 0.25$ and carry out calculations for OQRs with $E = 10$, 15 and 20. The results, see Fig. 5, show that when E increases, Ω^{max} gets bigger. This, see Eq. (4), happens due to two reasons: (i) Ω and Q_c are proportional to each other and (ii) Q_c, according to Eq. (5), increases with E. These two reasons imply that Ω increases with E and that the increase is almost linear. Theoretically, this result is deduced by combining Eqs. (4) and (5) and checking the linear dependence of the two functions on E. Moreover, we find that $\varepsilon^\dagger$ gets smaller when E gets bigger. We highlight that the behavior of

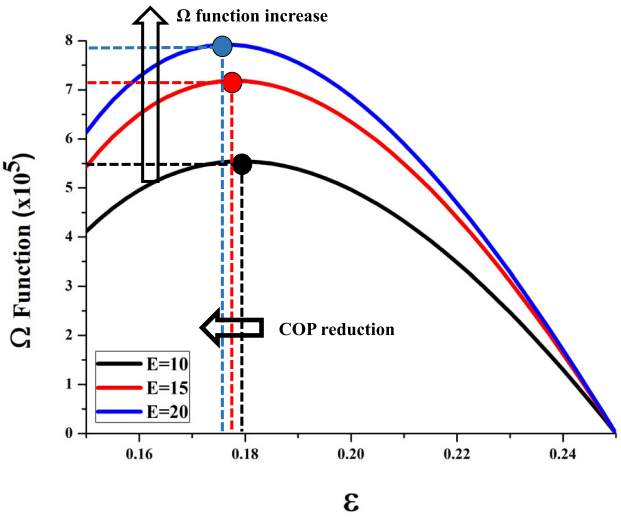

Fig. 5 Ω calculated for three different OQRs having $\varepsilon_C = 0.25$. In one of the OQRs, $E = 10$ (black line), in another, $E = 15$ (red line) and in the third one, $E = 20$ (blue line)

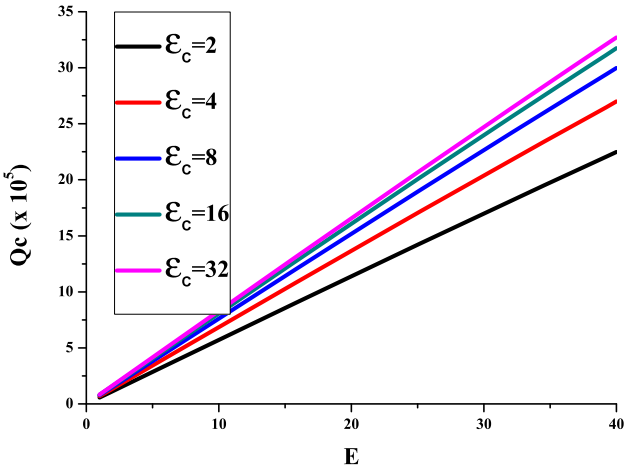

Fig. 6 Maximum cooling power Q_c^{max} versus E. We present results corresponding to $\varepsilon_C = 2$, 4, 8, 16 and 32. We use $T_h = 10$ and $\Gamma_h = \Gamma_1 = 10^{-3}$

$\varepsilon^\dagger$ with E is similar to the one found for ε^* with the energies of the qubits as the two functions are related. This result is logical due to the proportionality existing between Q_c and Ω once T_h and T_c are fixed, a result that can be theoretically checked using Eq. (4).

2.2 Optimizations for different E

Once we have optimized OQRs for fixed configurations of the hot and cold baths (i.e., for fixed combinations of the values of T_h and T_c), we perform a more general optimization changing the energy E of the qubit. In order to present the results in the best way, we perform calculations for several values of ε_C, i.e., for different combinations of T_h and T_c.

The optimizations are done now using the following protocol: (i) We choose ε_C, and we fix $T_h = 10$. (ii) We carry out calculations for several different qubit energies E. For each pair E, ε_C, we calculate

$$T_c = \frac{\varepsilon_C}{1+\varepsilon_C} T_h. \tag{9}$$

(iii) Then we do a loop of the possible values of ε calculating, for each QR, Q_c and Ω. (iv) We seek the biggest values Q_c^{max} and Ω^{max} of Q_c and Ω. Upon finding them, we also obtain ε^* and $\varepsilon^\dagger$. (v) Then we plot Q_c^{max}, Ω^{max}, ε^* and $\varepsilon^\dagger$ as functions of E. Finally, we change to another E and repeat steps (i)–(v), thus obtaining information for the chosen value of ε_C. Finally, we start the procedure again and repeat steps (i)–(v) for a new value of ε_C. To do the optimization process as complete as possible, we perform calculations for $\varepsilon_C = 2$, 4, 8, 16 and 32.

Figure 6 shows that Q_c^{max} increases linearly with E for every value of ε_C (see the lines of different colors in the figure). Thus, every time that we change ε_C, the slope of the line defining Q_c^{max} in terms of E changes, thus revealing that Q_c^{max} depends linearly on E as is deduced from Eq. (5).

We present, in Fig. 7, ε^* in terms of E to check how the COP corresponding to the best cooling power changes with E. The figure reveals two behaviors: (i) When ε_C is fixed, ε^* is a constant function that does not change with E, being this behavior independent of the concrete value of ε_C used in the calculation. We highlight that, for every ε_C, a small reduction of the value ε^* happens if

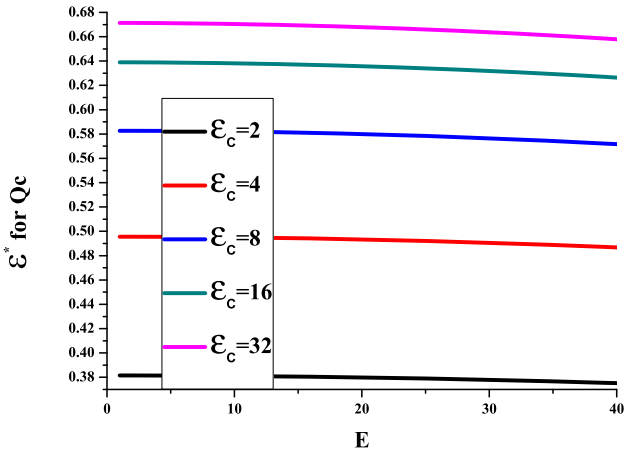

Fig. 7 COP corresponding to Q_c^{max} versus E. We present results corresponding to $\varepsilon_C = 2$, 4, 8, 16 and 32. We use $T_h = 10$ and $\Gamma_h = \Gamma_1 = 10^{-3}$

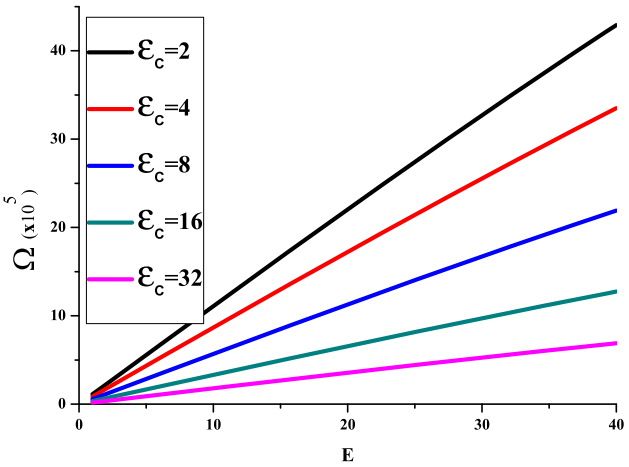

Fig. 8 Ω versus E. We present results corresponding to $\varepsilon_C = 2$, 4, 8, 16 and 32. We use $T_h = 10$ and $\Gamma_h = \Gamma_1 = 10^{-3}$

$E > 20$. This means that the value of E almost does not affect the optimization of Q_c and that only for very big values of E, small reductions of Q_c that are smaller than 1% are found.

Let us now study the behavior of Ω with E for different fixed values of ε_C. Figure 8 shows that Ω increases linearly with E, being this behavior independent of ε_C (i.e., of the temperatures of the two heat reservoirs). We note the similarity of this result to the one found studying the relation between Q_c and E. However, the results are not completely equal, being the major difference between them is the behavior found when ε_C is changed. Thus, we find that the slope of the curve Q_c vs. ε increases with ε_C and that the slope of the curve Ω vs. ε decreases upon increasing ε_C.

Finally we check how $\varepsilon^\dagger$ changes with E. The results of the study are found in Fig. 9, where we include results for $\varepsilon_C = 2$, 4, 8, 16 and 32. We observe that $\varepsilon^\dagger$ does not change with E for anyone of the ε_Cs. This means that different OQRs with distinct values of E work having the same Ω-regime. This result is very important, as it assesses the stability of OQRS working on the best Ω-regime when E is changed.

3 OQRs working in the high-temperature limit: a semiclassic model

Let us now study the performance of OQRs that work connected to heat reservoirs satisfying $T_h \gg E$ and $T_c \gg E$. In this limit, the OQR seems to be a classic refrigerator, but it is slightly different to them as some of its parameters still depend on E. Moreover, this limit is very interesting since, in it, the coupling between the qubit and the bath is necessarily small [43, 44], what asses the solution for Q_c found in Sect. 2 to be valid. So, the result is a heat engine that works by following the classic rules but that has a quantum reminiscences inside.

The semiclassic model of the OQR is depicted in Fig. 10. As we see, the form of the refrigerator is purely classic. It has two heat reservoirs of temperatures T_h and T_c on its extremes and a middle heat reservoir of temperature T_1. In this semiclassic refrigerator, $T_1 \geq T_h \geq T_c$, as is explained in [20]. Moreover, between the reservoirs of temperatures T_1 and T_h, a thermal resistance $R = \Gamma E/(4T_h)$ exists; we remark the dependence of the resistance on E, being this factor what links the new device with its quantum origins. Following the results of previous works [36, 39], we obtain the energy flux at the hot side of the engine.

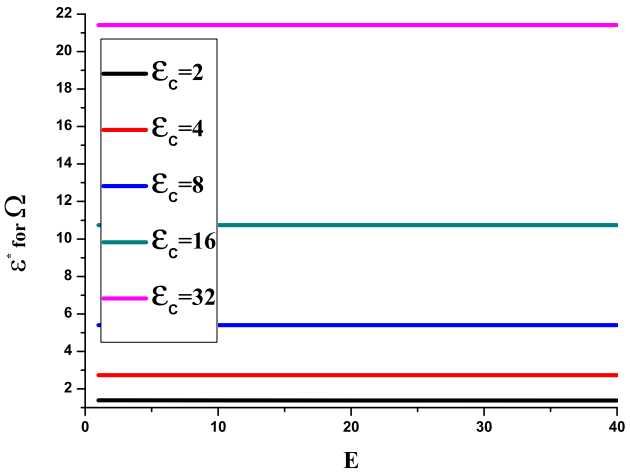

Fig. 9 COP corresponding to Ω^{max} versus E. We present results corresponding to $\varepsilon_C = 2, 4, 8, 16$ and 32. We use $T_h = 10$ and $\Gamma_h = \Gamma_1 = 10^{-3}$

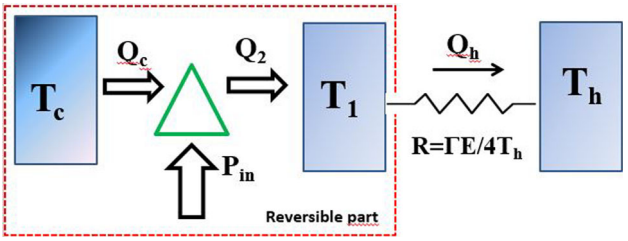

Fig. 10 Semiclassic version of the one-qubit quantum refrigerator (OQR). On the hot extreme, the conduction happens through a classic resistance R. R is defined in terms of the parameters of the OQR shown in Fig. 1

$$Q_h = \frac{\Gamma E}{4T_h}(T_1 - T_h) = K_h(T_1 - T_h). \tag{10}$$

Equation 10 shows that the amount of energy passing from the bath of temperature T_1 to that of temperature T_h depends linearly on the difference $T_1 - T_h$ and that the coefficient defining the heat K_h depends on E, the energy of the qubit. This means that, although the classic OQR seems to work as a classic refrigerator, the internal parameters defining it still preserve their quantum nature and depend on the quantum parameters: Γ, and E. Note that we have stated that K_h is a constant, and in fact, it is for each OQR since when we define K_h, we set the values of Γ and E. Finally, it is important to note that $Q_h > 0$ because $T_1 > T_h$, as explained in Calvo's et al. work [20].

Once we have Q_h, we calculate Q_c and Ω. Q_c is obtained using the reversibility condition of the CR at the heart of the engine. For the semiclassic OQR, this condition is written down as $Q_1/T_1 = Q_c/T_c$, and when it is used to calculate Q_c, we obtain

$$Q_c = \frac{\varepsilon}{1+\varepsilon}\frac{\Gamma E}{4T_h}(T_1 - T_h) \tag{11}$$

using now the energy conservation principle, we obtain,

$$P_{in} = \frac{1}{1+\varepsilon}\frac{\Gamma E}{4T_h}(T_1 - T_h). \tag{12}$$

We highlight the use of $\varepsilon = T_c/(T_1 - T_c)$ in Eqs. (11) and (12) instead of T_1 and T_c for commodity.

Employing now Eq. (4), we find

$$\Omega = \frac{\Gamma E T_c}{4T_h}(1 - T_h/T_c)\frac{2T_h - T_1 - T_c}{T_h - T_c}. \tag{13}$$

Let us now optimize Q_c, P_{in} and Ω to better understand the functioning of the high-temperature semiclassic OQR.

1. We first do the derivative of Q_c to T_1 to obtain

$$\frac{dQ_c}{dT_1} = \frac{\gamma E T_c}{4T_h}\frac{T_h}{T_1^2} \tag{14}$$

dQ_c/dT_1 is a positive function for every value of T_1. This means that Q_c has no extremes and it is a function that only grows with T_1. It cannot be used to optimize the semiclassic OQR. This result proves that OQRs and semiclassic OQRs work somehow differently. Note that in previous sections, we have proven that in OQRs, Q_c is a function that can be used to optimize OQRs.

2. The derivative of P_{in} is

$$\frac{dP_{in}}{dT_1} = \frac{\Gamma E}{4T_h}\left[1 - \frac{T_h T_c}{T_1^2}\right]$$

Doing $dP_{in}/dT_1 = 0$, we find $T_1^* = \sqrt{T_h T_c}$. This value of T_1 has no physical meaning since $T_1^* < T_h$, and by definition of the OQR and the semiclassic OQR, we have $T_1 > T_h$ (see Figs. 1 and 10). This means that P_{in} cannot be used to optimize the semiclassic OQR.

3. The derivative of Ω is

$$\frac{d\Omega}{dT_1} = \frac{\Gamma E T_c}{4T_h(T_h - T_c)}\left(\frac{2T_h + T_h T_c}{T_1^2} - 1\right) \tag{15}$$

Doing $d\Omega/dT_1 = 0$, we obtain $T_1^\dagger = \sqrt{2T_h^2 + T_h T_c}$. As $T_1^\dagger > T_c$ and $T_1^\dagger > T_h$, this temperature has physical meaning in our semiclassic OQR and can be used to optimize its performance. For $T_1^\dagger$, the cooling power $Q_1^\dagger$, expressed as function of ε_C, is

$$Q_c^\dagger = \frac{\Gamma E T_c}{4}\frac{\varepsilon_C}{\varepsilon_C + 1}\frac{\sqrt{2 + 3\varepsilon_C} - \sqrt{1 + \varepsilon_C}}{\sqrt{2 + 3\varepsilon_C}} \tag{16}$$

We note that this is the cooling power calculated at the maximum Ω regime. We note that for every ε_C, $Q_c^\dagger > 0$.
We also obtain $P_{in}^\dagger$, the power absorbed by the CR when the OQR works at its best Ω,

$$P_{in}^\dagger = \frac{\Gamma E}{4}\frac{\sqrt{(\varepsilon_C + 1)(2 + 3\varepsilon_C)} - \varepsilon_C}{\sqrt{(\varepsilon_C + 1)(2 + 3\varepsilon_C)}} \tag{17}$$

We notice that $P_{in}^\dagger > 0$ as expected, indicating that an optimal Ω-regime of work exists for the semiclassic OQR.

4 Concluding remarks

This work extends previous ones done on the optimization of qubit-based heat engines considering, for the first time, a one-qubit quantum refrigerator. Thus, we prove the utility of the methods proposed in [36–39] to study quantum heat engines beyond heat engines.

In the first part of the work, we have obtained the energy fluxes Q_c and Q_h of the quantum refrigerator, its Ω-function and the power P_{in} that it absorbs as functions of the parameters defining the engine. Then we have optimized the refrigerator working properties to the case where the temperatures of the hot and cold reservoirs are fixed. We found that for each pair of temperatures T_h and T_c, the cooling power is optimized for a temperature $T_1^* > T_h$ and that the value of T_1^* depends on T_h, T_c, the coupling parameters defining the engine, and E. Concretely, we found that T_1^* increases with E. We have also studied the Ω-function to discover that it is also optimized for a $T_1^\dagger \neq T_h,\ T_c$. We found that $T_1^\dagger > T_h$ and that it changes with E and with the coupling parameters defining the OQR. We also found that Ω increases when we increase E. It is important to remark that in OQRs, the Ω-function has a maximum for a concrete value of ε, while the Ω-function of classic RE does not have it.

In the last part of the article, we studied the semiclassic limit of one-qubit quantum refrigerators where $T_h \gg E$ and $T_c \gg E$. We found that in this limit, the refrigerator reduces to a classic one, but that some of the parameters defining that *classic refrigerator* depend on the energy of the qubit and the thermal couplings. That is, although the machine is now classic, its functioning still depends on its quantum nature. Optimizing the semiclassic version of the refrigerator, we found that: (i) Q_c cannot be used to carry out optimizations. (ii) P_{in} is optimized for a temperature that has no physical meaning, so it cannot be used to optimize the machine either. (iii) Ω is optimized for a temperature $T_1^\dagger$ that only depends on T_h and T_c and not on E, Γ_h or Γ_1. Result (iii) is very relevant as it proves that the semiclassic version of the OQR is optimized in the same way as a classic refrigerator does when the optimization is done using Ω, but that if Q_c is used, the semiclassic OQR no longer optimizes as a classic refrigerator.

Our work extends previous work on qubit-based quantum thermal machines by considering the optimization of the quantum and semiclassic versions of a classic single thermal resistance cooler. It proves that there are differences in the results of the optimizations that depend on the nature (quantum/classic) of the system. It also allows us to understand that even in the semiclassic limit, the optimizations lead to results that are somehow different to those obtained in classic refrigerators.

Acknowledgements The author thanks the UNED for providing its computational facilities to carry out the work. The author acknowledges the Ministerio de Ciencia e Innovación for financial support through the research project PID-2019-105182GB-I00.

Author contributions JJF contributed to all the steps concerning the elaboration of this manuscript.

Funding Open Access funding provided thanks to the CRUE-CSIC agreement with Springer Nature. Funding was received from the Ministerio de Ciencia e Innovación through the research project PID-2019-105182GB-I00.

Data availability This manuscript has no associated data added to any data repository. No data are associated in this manuscript.

Declarations

Conflict of interest The author declares that he has no conflict of interest.

Consent to participate The author manifests his consent to participate in this work.

Consent to publication The author manifests his consent for publication.

References

1. J. Gemmer et al. Quantum thermodynamics: emergence of thermodynamic behaviour within composite quantum systems, Lect. Notes Phys. **784** Berlin, Heidelberg (2009)
2. H.T. Quan, Y.-X. Liu, C.P. Sun, H. Nori, Phys. Rev E **76**, 031105 (2007)
3. H.T. Quan, Phys. Rev E **79**, 041129 (2009)
4. M.O. Scully, M.S. Zubairy, G.S. Argawal, H. Walther, Science **299**, 862 (2003)
5. M.O. Scully, K.R. Chaplin, K.E. Dorfman, M.B. Kim, A. Svidzinsky, Proc. Natl. Aca. Sci. USA **108**, 15097 (2011)
6. K.E. Dorfmann, D.V. Voronine, S. Mukamel, M. O. Scully **110**, 2746 (2013)
7. B. Lin, J. Chen, Phys. Rev E **67**, 046105 (2003)
8. M. Polettini, G. Verley, M. Esposito, Phys. Rev. Letter **114**, 050601 (2015)
9. P. Chambadal, *Les centrales Nucléaires* (Paris. France, Armand Colin, 1957), pp. 41–48
10. F.L. Curzon, B. Ahlborn, Efficiency of a Carnot engine at maximum power output. Am. J. Phys. **43**, 22 (1975)
11. A. De Vos, *Endoreversible thermodynamics of solar energy conversion* (Oxford University Press, Oxford, 1982)
12. F. Angulo-Brown, An ecological optimization criterion for finite-time heat engines. J. App. Phys. **69**, 7465 (1991)
13. S. Velasco, J.M.M. Rocco, A. Medina, A. Calvo-Hernández, Phys. Rev. Lett. **78**, 3241 (1997)
14. L. Chen, C. Wu, F. Sun, Finite time thermodynamic optimization or entropy generation minimization of energy systems. J. Non-Equilib. Thermodyn. **24**(4), 327 (1999)
15. A. Bejan, Entropy generation minimization: the new thermodynamics of finite size and finite time processes. J. Appl. Phys. **79**, 1191 (1997)
16. A. Calvo-Hernández, J.M.M. Rocco, S. Velasco, A. Medina, Irreversible Carnot cycle under per-time unit efficiency optimization. Appl. Phys. Lett. **73**(6), 853–855 (1998)
17. F. Angulo-Brown, L.A. Arias-Hernández, R. Páez Hernández, A general property of non-endoreversible thermal cycles. J. Phys. D: Appl. Phys. **32**, 1415 (1999)
18. D. Jou, J. Casas-Vazquez, G. Lebon, *Extended irreversible thermodynamics* (Springer, Berlin, 2000)
19. S. Velasco, J.M.M. Roco, A. Medina, J.A. White, A. Calvo-Hernandez, Optimization of heat engines including the saving of natural resources and the reduction of thermal pollution. J. Phys. D: Appl. Phys. **33**, 355 (2000)
20. A.C. Hernández, A. Medina, J.M.M. Roco, J.A. White, S. Velasco, Unified optimization criterion for energy converters. Phys. Rev. E **63**(3), 037102 (2001)
21. D. Ladino Luna, Effficiency of a Curzov Ahlborn engine with Dulong and Petit heat transfer law. Rev. Mex. Fis **48**(6), 86 (2002)
22. R. Paéz, F. Angulo-Brown, M. Santillán, Dynamic robustness and thermodynamic optimization in a non-endoreversible Curzon-Ahlborn engine. J. Non-Equil. Thermodyn. **31**(2), 173 (2006)
23. M. Feidt, Optimal use of energy systems and processes. Int. J. Exergy **5**(5/6), 500 (2008)
24. M.A. Barranco, N. Sánchez Salas, F. Angulo Brown, On the optimum operation conditions of and endoreversible heat engine with different heat transfer laws in the thermal couplings. Rev. Mex. Fis. **54**(4), 284 (2008)
25. S. Sieniutycz, S. Jezowsky, *Energy optimization in process systems* (Elsevier, Oxford, 2009)
26. M. Feidt, Themodynamics applied to reverse cycle machines, a review. Int. J. Refriger. **33**(7), 1327 (2010)
27. N. Sánchez-Salas, L. López-Palacios, S. Velasco, A. Calvo Hernández, Optimization criteria, bounds, and efficiencies of heat engines. Phys. Rev. E **82**, 051101 (2010)
28. B. Andresen, Current trends in finite-time thermodynamics. Andgewandte Chemie Int. Edn. **50**(12), 2690 (2011)
29. S. Sieniutycz, S. Jezowsky, *Energy optimization in process systems and fuel cells* (Elsevier, Oxford, 2013)
30. J. Gonzalez-Ayala, F. Angulo-Brown, A. Calvo-Hernández, S. Velasco, On reversible, endoreversible, and irreversible heat device cycles versus the Carnot cycle: a pedagogical approach to account for losses. Eur. J. Phys. **37**, 045103 (2016)
31. X.L. Huang, T. Wang, X.X. Yi, Effects of reservoir squeezing on quantum systems and work extraction. Phys. Rev. E **86**, 051105 (2012)
32. J.P. Pekola, Towards quantum thermodynamics in electronic circuits. Nat. Phys. **11**, 118 (2015)
33. F. Binder, S. Vinjanampathy, J. Goold, Enhancing the charging power of quantum batteries. Phys. Rev. E **91**, 032119 (2015)
34. S. Su, Y. Ma, J. Chen, C. Sun, The heat and work of quantum thermodynamic processes with quantum coherence. Chin. Phys. B **27**, 060502 (2018)
35. W. Niedenzu, V. Mukherjee, A. Ghosh, A.G. Kofman, G. Kurizki, Quantum engine efficiency bound beyond the second law of thermodynamics. Nat. Commun. **9**, 165 (2018)
36. J. Du, W. Shen, X. Zhang, S. Su, J. Chen, Quantum-dot heat engines with irreversible heat transfer. Phys. Rev. Res. **2**, 013259 (2020)
37. J.J. Fernández, Optimization of energy production in two-qubit heat engines using the ecological function. Quant. Sci. Technol. **7**, 035002 (2022)
38. J.J. Fernández, Energy production in one-qubit quantum Agrawal machines. J. Non-Equil. Thermodyn. **48**(3), 303 (2023)
39. J.J. Fernández, Unified trade-off optimization of one-qubit Novikov heat engines. Eur. Phys. J. Plus **138**, 778 (2023)

40. T. Chen, V. Balanchandran, C. Guo, D. Polleti, Steady state quantum transport through an anharmonic ocillator strongly coupled to two heat reservoirs. Phys. Rev. E **102**, 012155 (2020)
41. T. Chen, D. Polleti, Thermodynamic performance of a periodically driven harmonic ocillator correlated with the baths. Phys. Rev. E **104**, 054118 (2021)
42. M. Kaneyasu, Y. Hasewaga, Quantum Otto cycle under strong coupling. Phys. Rev E **107**, 044127 (2023)
43. A. Roulet, S. Nimmrichter, J.M. Arrazola, S. Seah, V. Scarani, Autonomous rotor heat engine. Phys. Rev E **95**, 062131 (2017)
44. S. Seah, S. Nimmrichter, V. Sacarani, Refrigeration beyond weak internal coupling. Phys. Rev. E **98**, 012131 (2018)
45. D. Manzano, A short introduction to the LIndbland máster equation. AIP Advances **10**, 025106 (2020)
46. J.D. Barrow, *The constants of Nature, from α to ω*: *The Numbers that Encode the Deepests Secrets of Universe* (Pantheone, New York 2002)
47. N. Sánchez-Salas, S. Velasco, A. Calvo-Hernández, Unified working regime of irreversible Carnot-like heat engines with nonlinear heat transfer laws. Energ. Convers. Management **43**, 2341 (2002)